

Advanced Signal Sensing Method With Adaptive Threshold Curve Based on Time Frequency Domain Reflectometry Compensating the Signal Attenuation

SEUNG JIN CHANG  (Member, IEEE)

Department of Electrical Engineering, Hanbat National University, Daejeon 34158, South Korea

This work was supported by the National Research Foundation of Korea grant funded by the Korea government (MSIT) under Grant NRF-2018R1C1B5086489.

ABSTRACT Adaptive fault detection method, which is compensating the wave attenuation along the propagation, is proposed in this article. Long cable system installed in the factory need to develop precise fault detection method considering propagation dispersion. Using the derived time delay between the incident and reflected wave which is generated from the fault, fault can be localized. The time-frequency cross correlation (TFCC) is a signal scanning process based on the similarity of the energy spectrum for detecting the reflected signal mixed with the noise. The threshold value in TFCC is a reference constant value for judging whether or not a fault is present. Due to the attenuation and dispersion of signal along the propagation, a new threshold value function considering attenuation and dispersion is needed. We propose the adaptive threshold curve for compensating the signal attenuation. We design the equivalent circuit of target cable (7 m length) and optimal reference signal based on the comparative analysis between the results of computer simulation and actual experiments of 7 m length cable. Based on the designed equivalent circuit of target cable(7 m length), a long cable system is modeled by simulation and the performance of the proposed method is proved through the simulation under the various noise level environments.

INDEX TERMS Advanced signal processing, signal sensing, signal detection, fault detection, adaptive curve, time-frequency domain reflectometry, health monitoring.

I. INTRODUCTION

As the factory automation soared, the machine began to connect with each other via cables. That is, the cable system in the automation factory is complicated. The condition of cable system of factory/power grid is the most important factor which can be considered as the blood vessel in body. Also, the wires inside the robot arm are complicated and easily broken, and the wire failure inside the robot arm cannot be easily detected because it is invisible [1]. Likewise, the failure of cable induce the much of economic damage in factory system. It is important to accurately measure the fault location. Especially, for a complex system where multiple faults occur or long cable system, precise fault location algorithm is important to prevent economic loss [2], [18]. In factory cable system and power grid cable system such as HVDC submarine/HTS cable system case, a lot of portion of repair cost depends on fault

localization time [2]. For this reason, fault localization accuracy is the core part for health monitoring algorithm. Many studies on fault localization have been conducted. Among these studies, reflectometry methods, which are mostly common used methods for fault localization, can be categorized by TDR (time domain reflectometry), FDR (frequency domain reflectometry), and TFDR (time frequency domain reflectometry) depending on the reference signal [3]–[7]. TDR and FDR use the step pulse and sinusoidal pulse defined in single domain.

On the contrary to this, TFDR uses the chirp pulse which is defined in time and frequency domain. In order to find out the fault location, it is necessary to perform a process of scanning the reflected signal generated from the fault location based on similarity with the reference signal. In a single domain, it is difficult to distinguish between the reflected signal and noise.

In order to easily detect the reflected signal from the signal mixed with the noise, reference signal used in TFDR method is designed in both domain. Especially, when the propagation distance is long or multiple reflections occur, TFDR method can be usefully applied. In lossy medium, the signal distortion and attenuation occur along the propagation. In TFDR method, we use TFCC (time frequency cross correlation) function to detect the reflected signal based on the similarity between reference and reflected signals. The distortion due to the propagation in lossy medium hinders the detection of similarity [8]–[14]. The threshold value in TFCC is a criterion for detecting and localizing the reflected signal mixed with noise. In conventional TFDR method, the threshold value is set to constant without the mathematical basis, because the exact TFCC value cannot be derived mathematically considering attenuation and dispersion [11]. However, the threshold value depends on the degree of distortion and propagation distance. Also, TFCC peak value at long-distance is too small to be classified between TFCC peak value of noise. In this case, the adaptive threshold curve would be standard whether the signal is reflected signal or noise.

In this paper, we focus the relationship between the TFCC value and propagation distance. To derive the TFCC value by the equation for propagation distance, we assume that the target cable is dispersionless media. However, we design the equivalent circuit of target cable considering the dispersion and attenuation. That is, we conduct the experiments under the actual environments. To design the equivalent circuit of target cable, we set the parameters by comparing the waveform acquired from the 7 m length target cable with those obtained by simulation. TFCC value of noise has a small value, so the TFCC value at long-distance signal can be confusing with the noise level. To verified the performance of distinguishing the noise and signal over long distance, we design the simulations in various noise environments. Based on the equivalent circuit of 60 m long target cable, we conduct the experiments on long cable by simulation.

II. THEORETICAL BACKGROUND

A. TIME-FREQUENCY DOMAIN REFLECTOMETRY

In this paper, TFDR method is introduced to detect the fault in cable. The incident signal is applied to the target cable and the reflected signal is generated at the impedance discontinuities point by radar theory. The mixed signals, which consist of incident, reflected signal, and noise, are acquired by the oscilloscope. After acquiring the mixed signals, we find out the reflected signal under other signals by using TFCC algorithm. We use the Gaussian linear chirp signal as the incident signal, and the incident signal is represented as follows [1]:

$$s(t) = \begin{cases} (A \cdot \frac{\alpha}{\pi})^{1/4} \cdot e^{-\alpha(t-t_0)^2/2 + j(\beta(t-t_0)^2/2 + \omega_0(t-t_0))}, & (t = 0 \leq t \leq T) \\ 0, & \\ \text{otherwise} & \end{cases}$$

where T is the duration of the incident signal, A is the amplitude of reference signal, α , β , t_0 , and ω_0 determine the time duration, frequency sweep rate, time center, and frequency center [8]. The reflected signal is expressed as follows:

$$r(t-d) = \eta \cdot \left(\frac{\alpha}{\pi}\right)^{1/4} \cdot e^{-\alpha(t-t_d)^2/2 + j(\beta(t-t_d)^2 + \omega_0(t-t_d) + \phi)}$$

where η is the magnitude of the attenuation coefficient at the travelling distance, and t_d is the time delay of the reflected signal. j and ϕ means imaginary part and phase shift of reflected signal. TFCC between the incident signal and the reflected signal is used to detect the reflected signal from mixed signals. TFCC is calculated by using the Wigner-Ville distribution and Wigner-Ville is expressed as follows [7]:

$$W(t, w) = \frac{1}{2\pi} \int s(t + \tau/2) s^*(t - \tau/2) e^{-jw\tau} d\tau \quad (1)$$

where $*$ means the conjugate operator and for calculation of complex signal, use the conjugate version of existing signal. Then the Wigner distribution of the reference signal $W_s(t, w)$ is derived as follows:

$$W_s(t, w) = \frac{1}{\pi} e^{-\alpha(t-t_0)^2 - (w-\beta(t-t_0)-\omega_0)^2/\alpha} \quad (2)$$

Based on the Wigner-Ville distribution, we detect the reflected signal from the incident signal using the similarities between incident and reflected signal, because the Wigner-Ville distribution is a kind of energy distribution. The normalized TFCC can be written as follows:

$$C_{sr}(t) = \frac{2\pi}{E_s E_r} \iint W_r(t, w) W_s(t' - t, w) dw dt' \quad (3)$$

The impedance discontinuities points can be located using the time delay between the peaks of the TFCC.

B. DEVELOPMENT OF THE ADAPTIVE THRESHOLD CURVE

The shielded cable, which is the path a wave propagates, reduce electrical noise from affecting the signal. According to this property, the inside of shielded cable can be considered as the dispersionless medium. The propagation constant, k , depends on the frequency. We design the reference signal as a narrow band signal so that the propagation constant can be expanded as Taylor series about w_o . The propagation constant $k(w)$ is expressed as following: $k(w) = k_o + k'_o(w - w_o) + \frac{1}{2}k''_o(w - w_o)^2 + \dots$ where, $k_o = k(w_o)$, $k'_o = (dk/dw)|_{w_o}$, and $k''_o = (d^2k/dw^2)|_{w_o}$. The propagation constant, $k(w)$, is real which means that we keep the k'_o and ignore the k''_o term. In the linear frequency-dependent attenuation, the phase velocity and group velocity of the wave are both equal and denoted by v . The Wigner distribution of the reflected signal $W_r(t, w)$ with velocity v can be obtained as follows:

$$W_r(t, w) = \frac{1}{\pi} e^{-\alpha(t-x/v)^2 - (w-\beta(t-x/v)-\omega_0)^2/\alpha} \cdot e^{-2Axw} \quad (4)$$

where, Aw is linearly approximation equation for frequency-dependent attenuation of medium, $\alpha(w)$. Based on (2), (3),

and (4) equations, we derive the TFCC function about propagation distance as following [8]:

$$C_{s,r}(t, x) = e^{-((\alpha^2+\beta^2)/2)(Ax)^2} \cdot e^{-((\alpha^2+\beta^2)/2)(t-x/v)^2} \quad (5)$$

where, x is the propagation distance. TFCC peak at long distance fault can be under the threshold value, so as to the reflected signal at long distance fault cannot be detected. TFCC value consists of two parts in (5). The first term is affected to the propagation distance and the second term indicates that the value increases according to the similarity of the signals. TFCC value depends on the second term in aspects of time. So as to this aspect, TFCC value will be maximum local peak at $t = x/v$ which means that the TFCC peaks positions indicate the center of transmitted signal. In other words, TFCC peaks values depends on the first term in the derived TFCC function, not second term. In this paper, we derive the adaptive threshold considering the propagation distance using the n' th reflected signal from the termination. The TFCC peak value using the derived TFCC function can be expressed as following:

$$C_{s,r}\left(\frac{pd}{v}, pd\right) = e^{-\frac{(\alpha^2+\beta^2)}{2}(A \cdot pd)^2} \cdot e^{-\frac{(\alpha^2+\beta^2)}{2}\left(\frac{pd}{v} - \frac{pd}{v}\right)^2} \quad (6)$$

where, d is the target cable length and p is the variable indicating the number of reflections. The second term in (6) goes to zero at multiple reflection signals. So, peak values in TFCC can be re-expressed as following:

$$TFCC_{\text{Peak}}(d) = e^{-((\alpha^2+\beta^2)/2)(A \cdot d)^2} \quad (7)$$

$$TFCC_{\text{Peak}}(2d) = e^{-((\alpha^2+\beta^2)/2)(A \cdot 2d)^2} \quad (8)$$

$$TFCC_{\text{Peak}}(3d) = e^{-((\alpha^2+\beta^2)/2)(A \cdot 3d)^2} \quad (9)$$

where, $TFCC_{\text{Peak}}$ is the peak value function and the peak values are the geometric sequence. In this paper, we propose the Threshold function, $T(p) = B(p^2)$. where, B is the peak value in TFCC at first reflection, $T(1) = B$. In future works, we develop the threshold function considering not cable termination but fault in middle of cable. Then, the adaptive threshold curves for each reflected signals from the termination and fault are needed to develop, since there are many reflected signals.

III. EXPERIMENTAL & SIMULATION RESULTS

A. EXPERIMENTAL SETUP AND RESULTS

To derive the adaptive threshold curve, we design the simulations considering the relation between the propagation distance and TFCC peak values. In this paper, we design the equivalent circuit of the HTS cable using the comparative analysis between the acquired signal from the actual 7 m HTS cable and designed circuit. After demonstrating the similarities between the simulation and experimental results, we verify the effectiveness of the proposed method through the simulation instead experiments. The adaptive threshold curve can be effectively used to detect long-distance fault, we select the HTS cable as a target cable, because the HTS cable is the promising power cable in future. And because

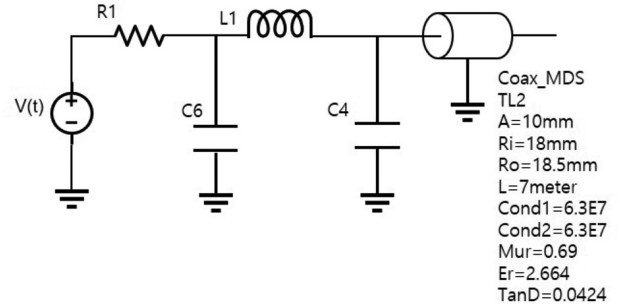


FIGURE 1. Equivalent circuit of the HTS cable.

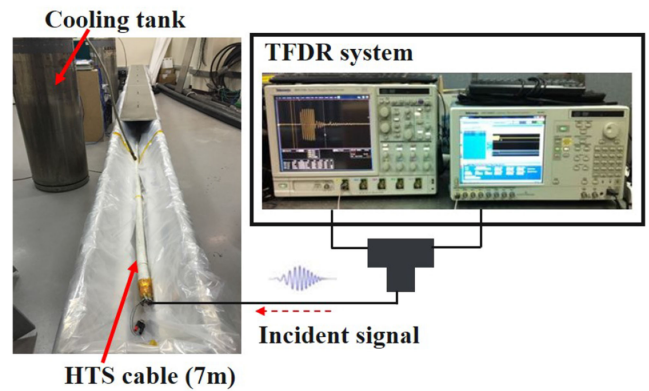


FIGURE 2. Experimental Setup of the 7 m length HTS cable.

it has low dispersion, HTS is suitable for verifying the performance of the derived adaptive threshold curve without the considering the dispersion. In this experiments, a single-phase 22.9 kV/50 MVA HTS cable (1G) with a length of 7 m is used. The difficulty of bending HTS cables makes it difficult to conduct experiments with long cable in laboratory. To cope with these difficulties, we design the equivalent circuit of the HTS cable using the comparative analysis between the acquired signal from the actual 7 m HTS cable and designed circuit. Fig. 1 shows the equivalent circuit using simulation tool. The experimental setup for the simulation is depicted in Fig. 2, and verifying the accuracy of the equivalent circuit by comparing between the acquired signals of simulation and experiments.

B. SIMULATION RESULTS

Based on the equivalent circuit through the experiments, we implemented the proposed experiments as a simulation circuit as following Fig. 3. In Fig. 3, we acquire the signal at the four points marked with red boxes. Fig. 4 illustrates the proposed experimental setup and we apply the reference signal to cable using the inductive coupler. The proposed system consists of two parts: (a) Arbitrary waveform generator (AWG), digital phosphor oscilloscope (DPO), (b) target cable. The AWG and DPO design and generate the incident signal, and acquire the transmitted signal through the inductive coupler installed at same distance, 20 m, respectively. After analyzing the frequency attenuation characteristics of target cable, we design

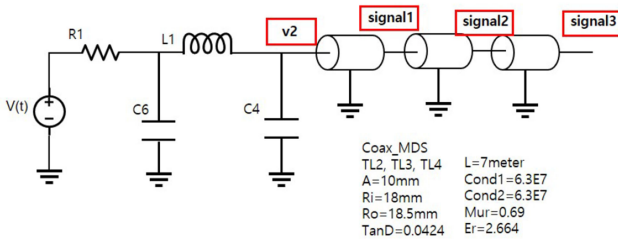


FIGURE 3. Equivalent circuit of the proposed experimental setup.

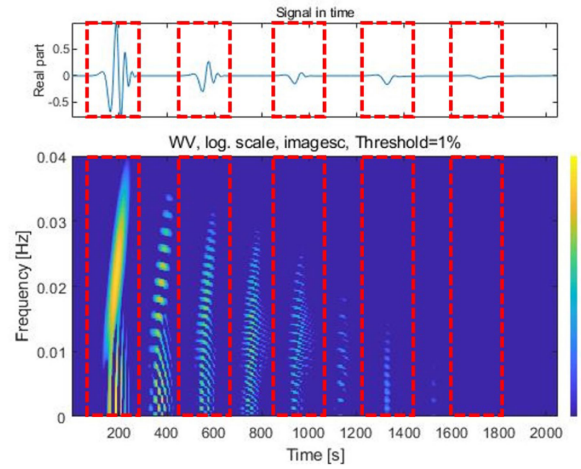


FIGURE 5. Wigner-Ville distribution of the acquired signal.

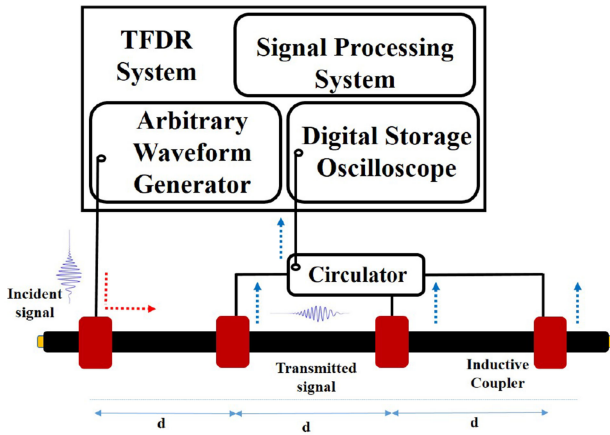


FIGURE 4. The proposed experimental setup.

the optimal parameters of reference signal. The optimal signal design process can be described as followings.

- Step 1: center frequency selection: f_0
- Step 2: frequency bandwidth selection: B
- Step 3: Time duration selection:

The optimal In reflectometry method, there is a blind spot which can be detected region. At this point, we first choose the target detection region and design the optimal signal which fits for the target region. In TFDR, the blind spot can be calculated as followings.

$$D_{\text{blind}} = 3\sigma v_{\text{pro}} = 3/(\sqrt{2}BW) \cdot v_{\text{pro}} \quad (10)$$

where D_{blind} , σ , v_{pro} , and BW is blind spot length [m], standard deviation of TFCC graph, propagation velocity, and bandwidth of signal. In this paper, we analyze the transmitted signal per 20 m, so we design the reference signal not to be overlapped between the TFCC graph of each signals as followings.

$$3/(\sqrt{2}BW) \cdot v_{\text{pro}}/2 = 20BW \approx 45 \text{ MHz} \quad (11)$$

In this paper, we select the parameters as follows: center frequency: 30 MHz, frequency bandwidth: 45 MHz, time duration: 90 ns. In the Fig. 5, we display the acquired signal and Wigner-Ville distribution. The red box indicates the incident & transmitted signals. As seen in the Wigner-Ville distribution, the transmitted signal and Wigner-Ville distribution at

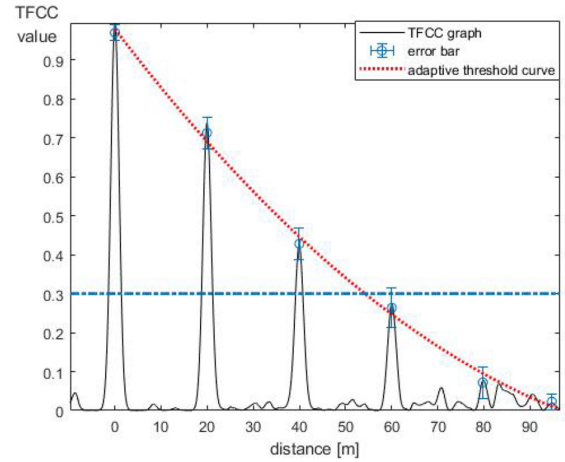


FIGURE 6. Simulation results with noise level [-0.1:0.1]: TFCC and adaptive threshold curve.

long distance is too small to be detected. The purpose of the simulation is to verify the feasibility of adaptive threshold curve. So as to, I conducted the experiments considering two factors: (1) attenuation degree along the propagation distance (2) noise level. The results of 3 kinds of experiments are shown graphically based on 100 times experiments per each, that is total 300 times experiments are conducted. As shown Figs. 6, 7, and 8, we add the various noise level for implementing the actual situation. Furthermore, the comparative analysis among the TFCC peak values at transmitted signals are shown in Figs. 6–8. (b). In Fig. 6, we add the noise [-0.1–0.1]. Since the noise affects the TFCC peak values, we calculated the mean and deviation of peak values from the TFCC graph we got 100 times. The adaptive threshold curve can be derived from the first peak value. The error bar depicts the deviation and mean of the TFCC peak values and the threshold curve is drawn within the range of the peak values. The TFCC graphs with the noise level 0.1, 0.2 and 0.5 are depicted in Figs. 6, 7

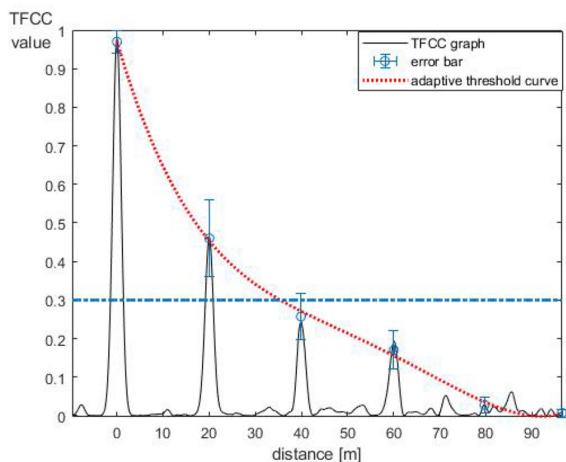


FIGURE 7. Simulation results with noise level [-0.2:0.2]: TFCC and adaptive threshold curve.

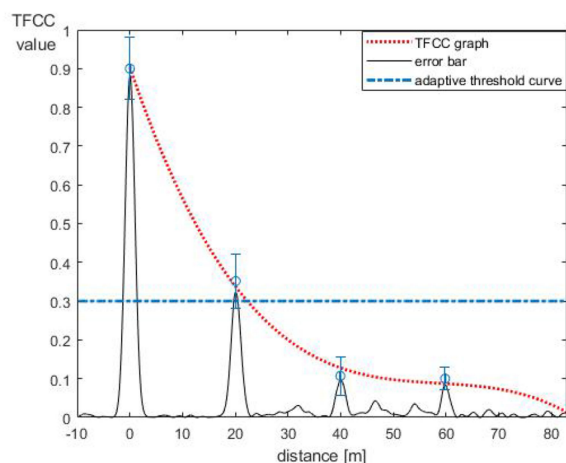


FIGURE 8. Simulation results with noise level [-0.5:0.5]: TFCC and adaptive threshold curve.

and 8, respectively. Through the comparative analysis according to the noise level, we can see the more noise, the larger deviation in TFCC graph and these points are shown in the error bar of each figure. Conventional TFDR method set the threshold as constant value 0.3. As for this constant threshold, the transmitted signal behind 40 m with the noise level 0.5 cannot be detected. We can verify that the fourth peak in Fig. 6, the third/fourth peak in Fig. 7 and the third/fourth peak in Fig. 8 can be detected by the adaptive threshold curve not conventional threshold value. Also, the peak value behind 80 m cannot be distinguished between other small peak values of noise. As the signal propagates, the signal becomes more severe in distortion, and when the TFCC peak values becomes smaller than a certain level, the detection reliability decreases. In the future works, we derive the probability relation equation between the propagation distance and TFCC considering the dispersion with the noise and model the fault reliability using reflection coefficient including phase term.

IV. CONCLUSION

To improve the performance of fault localization, we propose the adaptive fault detection method based on time-frequency domain reflectometry compensation the wave attenuation and dispersion. Using the time delay between the incident and reflected signal, the fault location can be calculated. The time-frequency cross correlation (TFCC), which is a scanning process for detecting the reflected signal from fault, is used to obtain the time delay. When the peak value of TFCC exceeds the constant threshold value, we judge there is a fault in target cable. In this paper, we derive the TFCC function along the propagation distance and model the adaptive threshold curve considering the attenuation along the propagation distance without dispersion. In this paper, we design the optimal signal which is suitable for the HTS cable and we design the equivalent circuit of HTS cable. Through the comparative analysis between the acquired signal from the actual 7 m length HTS cable and simulation, we verify the accuracy of simulation. Based on the verified simulation circuit, we designed an experiment to verify the adaptive threshold curve performance. The simulations with a variety of noise level also demonstrates a superiority of the proposed method over the conventional TFDR method. In future work, we are going to derive the probability relation equation between the propagation distance and TFCC considering the dispersion with the noise and model the fault reliability using reflection coefficient including phase term.

REFERENCES

- [1] S. J. Chang and J. B. Park, "Wire mismatch detection using a convolutional neural network and fault localization based on Time-Frequency-Domain Reflectometry," *IEEE Trans. Ind. Electron.*, vol. 66, no. 3, pp. 2102–2110, Mar. 2019.
- [2] G. Y. Kwon *et al.*, "Offline fault localization technique on HVDC submarine cable via Time-Frequency Domain Reflectometry," *IEEE Trans. Power. Deliv.* vol. 32, no. 3, pp. 1626–1635, Jun. 2017.
- [3] L. A. Griffiths, R. Parakh, C. Furse, and B. Baker, "The invisible fray: A critical analysis of the use of reflectometry for fray location," *IEEE Sensors J.*, vol. 6, no. 3, pp. 697–706, Jun. 2006.
- [4] C. Parkey, C. Hughes, and N. Locken, "Analyzing artifacts in the time domain waveform to locate wire faults," *IEEE Instrum. Meas. Mag.*, vol. 15, no. 4, pp. 16–21, Aug. 2012.
- [5] C. Furse, Y. C. Chung, R. Dangol, M. Nielsen, G. Mabey, and R. Woodward, "Frequency-domain reflectometry for on-board testing of aging aircraft wiring," *IEEE Trans. Electromagn. Compatib.*, vol. 45, no. 2, pp. 306–315, May 2003.
- [6] F. Auzanneau, "Wire troubleshooting and diagnosis: Review and perspectives," *Prog. Electromagn. Res. B.* vol. 49, pp. 253–279, 2013.
- [7] I. Luca *et al.*, "OMTDR based integrated cable health monitoring system SmartCo: An embedded reflectometry system to ensure harness auto-test," in *Proc. IEEE. Int. Conf. Indus. Electron. Appl.*, 2015, pp. 1761–1765.
- [8] S. J. Chang and S. I. Moon, "Compensation for group velocity of polychromatic wave measurement in dispersive medium," *MDPI. Appl. Sci.*, vol. 7, no. 12, 2017, Art. no. 1306.
- [9] S. J. Chang *et al.*, "Condition monitoring of instrumentation cable splices using Kalman filtering," *IEEE Trans. Instrum. Meas.*, vol. 64, no. 12, pp. 3490–3499, Aug. 2015.
- [10] S. J. Chang, C. K. Lee, Y.-J. Shin, and J. B. Park, "Multiple resolution chirp reflectometry for fault localization and diagnosis high voltage cable in automotive electronics," *Meas. Sci. Technol.*, vol. 27, no. 12, pp. 1–5, Oct. 2016.

- [11] C. K. Lee *et al.*, “Diagnostics of control and instrumentation cables in nuclear power plant via time-frequency domain reflectometry with optimal reference signal,” in *Proc. 9th Int. Conf. Insulated Power Cables*, Versailles, France, 2015, Paper 9.
- [12] J. Wang, P. E. C. Stone, D. Coats, Y.-J. Shin, and R. A. Dougal, “Health monitoring of power cable via joint time-frequency domain reflectometry,” *IEEE Trans. Instrum. Meas.*, vol. 60, no. 3, pp. 1047–1053, Mar. 2011.
- [13] J. Wang, P. E. C. Stone, Y.-J. Shin, and R. A. Dougal, “Application of joint time-frequency domain reflectometry for electric power cable diagnostics,” *IET Signal Process.*, vol. 4, pp. 395–405, 2010.
- [14] Y.-J. Shin *et al.*, “Application of time-frequency domain reflectometry for detection and localization of a fault on a coaxial cable,” *IEEE Trans. Instrum. Meas.*, vol. 54, no. 6, pp. 2493–2500, Dec. 2005.
- [15] B. R. Mahafza, “*Radar Systems Analysis and Design Using MATLAB*,” 2nd ed. NW: Taylor & Francis Group, 2005.
- [16] L. Sommervogel, L. E. Sahmarany, and L. Incarbone, “Method to compensate dispersion effect applied to time domain reflectometry,” *IET Electron. Lett.*, vol. 49, no. 18, pp. 1154–1155, Aug. 2013.
- [17] H. M. Hashemian and W. C. Bean, “State-of-the-art predictive maintenance techniques,” *IEEE Trans. Instrum. Meas.*, vol. 60, no. 1, pp. 226–236, Jan. 2011.
- [18] J. P. Llinares, J. A. A.-Daviu, M. R. Guasp, M. P. Sanchez, and V. C. Alarcon, “Induction motor diagnosis based on a transient current analytic wavelet transform via frequency B-Splines,” *IEEE Trans. Ind. Electro.*, vol. 58, no. 5, pp. 1530–1544, Sep. 2010.



SEUNG JIN CHANG (Member, IEEE) was born in Seoul, South Korea. He received the B.S. and Ph.D. degrees from the Department of Electrical and Electronic Engineering, Yonsei University, Seoul, South Korea, in 2010 and 2017 respectively. Upon his graduation, he joined the School of Electrical and Computer Engineering, Seoul National University, as a Postdoctoral Researcher in 2018. He joined the Department of Electrical Engineering, Hanbat National University, Daejeon, South Korea, as an Assistant Professor in 2018. His current research interests are characterized by condition monitoring based on deep learning, diagnosis and prognostics of cables and batteries, applied signal processing techniques, and time frequency analysis.